Journal of Computational Applied Mechanics 2025, 56(1): 101-126

DOI: 10.22059/jcamech.2024.377272.1111

RESEARCH PAPER

Static Response of Laminated Plate Using New Parabolic Higher Order Shear Deformation Theory: A Finite Element Approach

Sumit Khare [a], Rahul Kumar [b], Harish K. Sharma [c], Ram Bilas Prasad [d], Kanif Markad [e, *], Suraj Singh [b], Ashutosh K. Tiwari [b], Sourabh Ven [f]

[a] *Department of Mechanical Engineering, SVNIT, Surat (GJ), India*
[b] *Department of Mechanical Engineering, IET, DDU, Gorakhpur, India*
[c] *Department of Mechanical Engineering, GLA University, Mathura, India*
[d] *Department of Mechanical Engineering, MMMUT, Gorakhpur, U.P, India*
[e] *Department of Mechanical Engineering, DVVP College of Engineering, Ahmednagar, India*
[f] *Department of Civil, Computer Science and Aeronautical Technologies Engineering, Roma Tre University, Via Vito Volterra 62, Rome, 00146, Italy*

Abstract

This study presents a new exponential higher-order shear deformation theory (NEHSDT) to examine the flexural analysis of multi-layered laminated composite plates. The novel parabolic shear deformation function is developed to analyze the bending response of laminated plates. A new shear deformation theory eliminates the need for shear correction factors. The present theory gives an exact parabolic distribution of transverse shear stress over the thickness and fulfills the traction-free boundary conditions on the outer surfaces of multi-layered laminated plates. The governing equations are solved using the finite element method. In this finite element method, a nine-nodded isoperimetric element with seven degrees of freedom per node is formed especially for this purpose. Illustrative examples are presented to demonstrate the predictive capability of the proposed finite element method. The presented numerical results are compared with the existing results to illustrate the correctness and robustness of the finite element method. The proposed analysis is accurate, converges rapidly, and is valid for thin and thick laminated plates based on comparisons with earlier higher-order shear deformation theories. In addition, the present results may be taken as the benchmark for further studies.

Keywords: HSDT; FEM; Laminated Plate; Stress distribution; Deflection

1. Introduction

Multi-layered structural composites such as sandwich and laminated plates are often utilized in engineering applications. Due to their wide range of applications, it is required to analyze multi-layered composite structures statically. Their applications are in aviation, marine, civil, rail routes, space structures, underwater submarines, polymer electronics, and different fields. These multi-layered composite materials can be used in harsh environments such as the deep sea to high elevations overhead. This extensive usage could be credited to the high stiffness/weight proportion and

* Corresponding author. *E-mail address:* kmarkad13@gmail.com

increased density-to-weight proportion. The composite material is enabled by the optimal ply orientation and thickness variation of plies to incorporate into harsh environments. These structures might be presented to extreme functional circumstances, such as extrinsic, time-dependent influences.

Consequently, it is pivotal to decide on the statics analysis of laminated plates and ensure that their excitation frequency is not greater than the natural frequencies. It is not a new topic to examine the linear static behavior of plates, remarkably isotropic rectangular plates. An in-depth analysis of free vibrations and bending under transverse loading for laminated plates are provided in the book by J M Whitney [1]. There have been a lot of publications recently about static analysis of rectangular and circular laminated plates [2, 3] Expanded utilization of high-tech materials in basic designs requires an Advanced and exact model-based theory to precisely anticipate the structural behaviour. The benefit of two-dimensional theories over three-dimensional theories is that they lower the dimension of the expressions employed in mathematical modelling, resulting in a significant reduction in computation time Khare and Mittal [4]. The researchers have taken a lot of consideration in analyzing the laminated composite and sandwich plates for many years. They proposed several plate theories. From these theories, the zigzag (ZZ), equivalent single layer (ESL), and layer-wise (LW) theories are commonly utilized for the thin plates structural analysis. Traditional plate theories were first established for homogeneous plates and thereafter extended to orthotropic and anisotropic plates.

The equivalent single-layer (ESL) [5, 6] and layer-wise (LW) [7] theories were proposed based on the two-dimensional characterization of structures to study plate as well as shell-type layered structures precisely and with less computational effort. ESL formulations are often less complex than LW formulations. They can be effortlessly executed in mathematical methods while giving exact displacements and stress results, particularly for thin and moderately thick laminated plates. The First ESL modeling was the classical laminated plate theory (CLPT). The CLPT is derived based on Kirchhoff's hypothesis. This theory is based on the transverse normality assumption and overlooks the transverse shear deformation [8]. After that, the first-order shear deformation theory (FSDT) was proposed according to Reissner [9] and Mindlin [10] which considers linear in-plane stresses and deformation and also relieve the normality constraint as well as accommodates constant transverse shear deflection. The plate's top and bottom surfaces have non-zero traction due to Higher-order shear deformation theories, including higher-order terms in Taylor's expansions of the displacements in the thickness coordinate, which were proposed to improve the performance of FSDT. HSDTs are later proposed, which assure shear stress-free boundary conditions at the outer surfaces and parabolic transverse stress fluctuation and provide precise stability analysis. The observations for thick laminates reveal that in-plane stresses are substantially better than those found by FSDT, although there are still inaccuracies compared to 3D models[11]. For the flexural analysis of cross-ply laminates, Idlib et al. [12] examined the CLPT [13] with the TSDT and the parabolic shear deformation theory (PSDT) [14] HSDTs containing five field variables are the most common for multi-layered laminated composites. Other HSDTs featuring more than five field variables and are attributed to the following properties: ease of execution, inexpensive calculation, and higher precision. Moreover, increasing the sequence of variation for axial displacements along the thickness does not enhance the representation of the behaviour of multilayered laminates appreciably. Hyperbolic, logarithmic, exponential, trigonometric, and algebraic shear deformation theories are among the nonpolynomial shear deformation theories (NPSDTs), consisting of nonpolynomial functions. The first nonpolynomial function was carried out by Levy [15] using the sinusoidal function to analyze thick isotropic plates. Several researchers have recently employed NPSDTs for the static analysis of laminated and sandwich composite plates [16], [17]. Among the NPSDTs, as mentioned above, the correctness of Grover's [18] inverse hyperbolic shear deformation theory (IHSDT) is also extensively documented in the literature [19]. The trigonometric function was carried out by Zenkour AM [20] , Mantari JL et.al [21], Grover N et.al [22], Soldatos [23] first employed a hyperbolic function to develop HSDT for composite plates. Hyperbolic function was later carried by El Meiche et al. [24], Akavci SS et al. [25], Grover N et al. [18] [26] [27] The exponential function was first used by Karama et al.[28] to develop a HSDT for composite beams. Later, Aydogdu [29], Mantari [30], Sarangan and Singh [31], and many others developed such exponential shear deformation theories. Reddy [32], Shimpi and Patel [33],Kim et al. [34], Mantari et al. [35] and many others contributed by presenting their algebraic transverse shear deformation theories.

However, to the best of the author's knowledge, several areas of bending analysis utilizing NPSDTs, such as antisymmetric cross-ply, have not been fully addressed in numerous ways. As a result, it is critical to correct these inconsistencies in the published literature for NPSDT. Several review papers on sandwich plates and laminated

composite have been published in the literature by different academics, including [36], [37] [38].

Many numerical approaches have been utilized in structural analysis. The finite element approach (FEM) is among the most widely used computational techniques for the examination of composite plates [39] [40, 41]. The FEM has unique benefits over other approaches when addressing complicated geometries and boundary conditions. Although conventional 3D finite elements may be used to evaluate laminated and sandwich plates, they may be computationally infeasible for modelling real-world conditions [42]. In FEM, the field is split into a definite number of elements. A limited set of variables determines an individual element's behaviour. The entire system may be solved as a collection of its elements using typical discrete problem approaches [43]. The main benefit of FEM is the discretization procedure. Fried et al. [44] proposed the smallest number of degrees of freedom for triangular elements to correctly account for shear stresses in thin plate bending. Dvorkin's Ph.D. thesis,[45] among other things, highlighted and clarified the shear locking problem more thoroughly. The displacement technique, which uses C^0 continuity and C^1 continuity Hermite estimates are commonly used in the finite element method. The C^0 On the other hand, finite element formulation is more often used due to its ease of implementation. Furthermore, the Hermite element is only supported by a few finite element systems. Only FEA Tool Multiphysics and Get FEM++ support Hermite elements among several easily available FE software[46]. Due to its widespread and deep-rooted mathematical basis, FEM is the most favoured technique for studying structural behaviour, as seen by the brief literature discussed above. To depict the bending, buckling, and vibration of structural composites in an efficient way, higher-order shear deformation theories are created to overcome the limits of classical laminated plate theory and first-order shear deformation theories. However, most of the sources mentioned above do not consider penalty constraints. Those who have thought about it haven't shown the impact of various penalty constraints. As a result, it's critical to research to determine the competence of the newly produced NEHSDT for stagnant analysis. The weak form of the governing equations is formulated using an energy technique. Generalized higher-order shear deformation theories (HSDT) are explored for kinematic modelling of the plate and then discretized using a nine-noded penalty-based C^0 finite element.

Recently many authors have work on variety of work on analysis of laminated , FGM , and sandwich plates Motezaker, et al. [47] used Newmark and Galerkin,for dynamic analysis induced by earthquake load in concrete pipes. Kolahchi, et al. [48]studied optimal dynamic properties of laminated sandwich multiphase nanocomposite truncated conical shell using differential quadrature method. Hajmohammad, et al. [49] used hyperbolic shear deformation beam theory for dynamic analysis in beam element. Al-Furjan, et al. [50]studied experimental analysis for the mechanical properties of 7075-T6 aluminum reinforced with SiC particles. Al-Furjan, et al [51] investigated wave propagation of micro-sandwich beams using refined zigzag theory . Kumar, et al. [52] used HSDT model for the nonlinear bending analysis of FGM plate. Nanocomposite piezoelectric-leptadenia pyrotechnica rheological elastomer-porous functionally graded materials micro viscoelastic beams at different strain gradient higher-order theories were studied for dynamic instability by Al-Furjan, et al [53]. Al-Furjan, et al [54] implemented first order shear deformation theory for the numerical analysis to assess how much energy is absorbed by vibrations in a conical, three-layered panel that is situated on a viscoelastic substrate. Al-Furjan, et al [55] studied frequency, damping, bending, and buckling of an embedded sandwich nanoplate utilizing the boundary shape function differential quadrature hierarchical finite element technique and several plate theories, including enhanced zigzag theory. Kumar, et al. [56] examined bending analysis of bidirectional FGM plate using meshfree approach. Under quasi-static loading, the impact of the hole notched in GLARE and GFRP composites is investigated by Chu, et al [57]. The framework is solved using the Newmark technique and the differential quadrature method (DQM) in order to obtain the flexural moment and dynamic deflection by Al-Furjan, et al [58]. For the circular sandwich plates, frequency analysis is carried out by Chu, et al [59] in the pre- and post-buckling regions, which resulted from an in-plane thermal field. Al-Furjan, et al [60] examined wave propagation and vibration of corrugated smart sandwich nanobeam via exact solution approach. Wan, et al. [61] investigated the effects of various parameters on the forced and free vibration characteristics, as well as the post-buckling behavior of a rhombic plate situated on a viscoelastic torsional frictional substrate. Al-Furjan, et al [62] examined wave propagation in micro air vehicle wings featuring a honeycomb core, covered with porous functionally graded material Chu, et al.[63]and nanocomposite magnetostrictive layers. Chu, et al. [63]studied energy harvesting and dynamic behavior of SMA nano conical panel via DQ-IQ-Newmark methods . Wan, et al. [64] examined the supersonic flutter behavior and reliability of smart hybrid nanocomposite trapezoidal plates, taking into account various practical factors.

The present paper deals with providing enough numerical approaches with the best displacement model to aid in the design of a final laminated composite product. The majority of aerospace, space research, and defense organizations aim to create low-cost, highly durable products for real-world hazards. Case studies may also result in a lighter design of laminated plates used in high-performance systems where weight reduction is critical, such as aeronautical, spaceship, and missile constructions. An accurate, stable, and effective new parabolic HSDT is proposed to predict the flexural analysis of laminated plates in the present work. The convergence and validation studies of the new HSDT model for various problems are carried out. It is noticed that the results obtained utilizing the current theory are in close agreement with the three-dimensional Quasis results reported in the literature.

2. Mathematical model design

A rectangular laminated structural composite plate composed of multi-layers placed in a specific order $\left(\theta_1 / \theta_2 / \theta_3 ..... / \theta_n\right)$ is utilized for analysis. The dimensions of the plate are length a, breadth b, and constant total thickness h. Fig.1 shows a cartesian coordinate system with the x-y plane coincident with the plate's central plane θ_n.

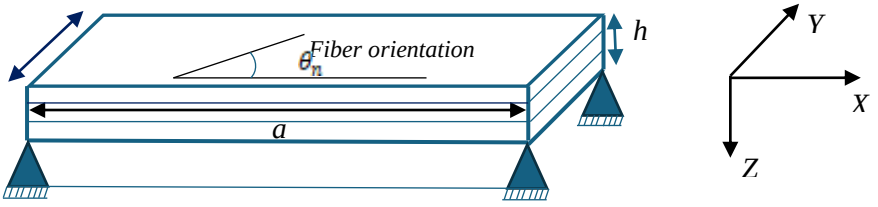

Fig 1. Laminate geometry with reference axes and fiber orientation

2.1. Displacement field model

The Lagrange basis function, which requires C^0 continuity of the field variables, is used in most FEM model which utilizes displacement. Approximating the solution for C^1 continuity using the Hermite function has its individual set of challenges in terms of FEM code implementation [65][57]. Artificial field variables must be used to create the FEM with HSDT (as per Eq. (1)) using the Lagrange element, which reduces the needed continuity to C^0. Penalty limits on the strain energy [66][58] shown in the next section compensate for this conversion. HSDT currently has seven field variables. Based on the above assumption. The displacement field of the present higher-order theory model can be written as

$$u = u_0 - z\frac{\partial \omega_0}{\partial x} + f\left(z\right)\theta_x\left(x,y\right) \tag{1}$$

$$v = v_0 - z\frac{\partial \omega_0}{\partial y} + f(z)\theta_y(x,y)$$

$$\mathrm{w} = w_0$$

u, v, w are the function of x, y, z and u_0, v_0 and w_0 are functions of x and y. Where, u, v, and w are the displacements of an arbitrary point in x, y, and z directions, respectively; u_0, v_0, and w_0 denote the midline displacements, respectively. θ_x And θ_y represent the shear deformation of the midplane normal about the *y* and *x*-axis, respectively. $f(z)$ is a transverse shear strain function of a thickness coordinate (z). Polynomial or nonpolynomial shear deformation theories, such as trigonometric, hyperbolic, and logarithmic, are named after the function involved in the mathematical formulation. Researchers are continually seeking new theories to improve the accuracy and stability of their results. In this pursuit, the authors of this paper have developed new exponential higher-order shear deformation theory aimed at providing better solutions. The $f(z)$ (NEHSDT) satisfy the zero transverse shear stress boundary condition at the top and bottom surfaces of the plate, eliminating the need for a shear correction factor. There are several

works of literature are there who utilize Algebraic, Trigonometric, Inverse trigonometric, Hyperbolic and Inverse hyperbolic, Exponential, and Logarithmic transverse shear strain functions so as to get optimized, better-validated results during structural analysis, which is depicted in Table 1 where the newly proposed theory is expressed as

$$f(z)=\left(\left(\sin\left(\frac{r\pi z}{h}\right)\right)e^{\cos\left(\frac{\pi z^2}{h}\right)}\right)-z\left(\left(r\pi e^{\cos\left(\frac{\pi h}{4}\right)}\right)\cos\left(\frac{r\pi}{2h}\right)-\left(\pi e^{\cos\left(\frac{\pi h}{4}\right)}\right)\sin\left(\frac{r\pi}{2h}\right)\sin\left(\frac{r\pi}{2}\right)\right)$$

Table 1. List of reported transverse shear strain functions.

Sr. No.	Transverse shear strain functions f (z)	Proposed by	Abbreviation
1	$\frac{z}{2}\left(\frac{h^2}{4}-\frac{z^2}{3}\right)$	[67]	**A-1**
2	$\frac{5z}{4}\left(1-\frac{4z^2}{3h^2}\right)$	[68]	**A-2**
3	$\left(z-\frac{4z^3}{3h^2}\right)$	[32]	**A-3**
4	$\frac{3}{2h}\left(z-\frac{4z^3}{3h^2}\right)$	[69]	**A-4**
5	$f(z)=\frac{9z}{8}-\frac{9z^3}{6h^2}$	[70]	**A-5**
6	$z\left(1-\frac{3}{2}\left(\frac{z}{h}\right)^2+\frac{2}{5}\left(\frac{z}{h}\right)^4\right)$	[71]	**A-6**
7	$p\left(\frac{z}{h}\right)^3-\frac{3p}{4h}z \quad p=0.9$	[72]	**A-7**
8	$\sin\left(\frac{\pi z}{h}\right)$	[73]	**T-1**
9	$\frac{h}{\pi}\sin\left(\frac{\pi z}{h}\right)$	[74]	**T-2**
10	$\tan(mz)-mz\sec^2\left(\frac{mh}{2}\right) \quad m=\frac{1}{5h}$	[21]	**T-3**
11	$z\sec\left(\frac{rz}{h}\right)-z\sec\left(\frac{r}{2}\right)\left[1+\frac{r}{2}\tan\frac{r}{2}\right] \quad r=0.1$	[22]	**T-4**
12	$\sin\left(\frac{mz}{h}\right)\cos\left(\frac{mz}{h}\right)-\left(\frac{mz}{h}\right)\cos(m) \quad m=2.5$	[31]	**T-5**

13	$\sin\left(\frac{2p\pi z}{h}\right)-\frac{2p\pi z}{h}\cos(p\pi)$ $p=0.6$	[72]	**T-6**
14	$h\tan^{-1}\left(\frac{rz}{h}\right)-\frac{16rz^3}{3h^2\left(r^2+4\right)}$ $r=1$	[75]	**IT-1**
15	$\tan^{-1}\left[\sin\left(\frac{\pi z}{h}\right)\right]$	[76]	**IT-2**
16	$-z+h\tan^{-1}\left(\frac{2z}{h}\right)$	[77]	**IT-3**
17	$\frac{h}{r}\tan^{-1}\left(\frac{rz}{h}\right)-\frac{z}{\left(\frac{r^2}{4}+1\right)}$ $r=2.5$	[78]	**IT-4**
18	$f\left(z\right)=h\tan^{-1}\left(\frac{z}{h}\right)-z\left(1-\frac{4z^2}{15h^2}\right)+ze^{-2\left(\frac{z}{h}\right)^2}$	[79]	**IT-5**
19	$h\sinh\left(\frac{z}{h}\right)-\mathrm{z}\cosh\left(\frac{1}{2}\right)$	[23]	**H-1**
20	$\frac{3\pi}{2}h\tanh\left(\frac{z}{h}\right)-\frac{3\pi}{2}z\sec h^2\left(\frac{1}{2}\right)$	[25]	**H-2**
21	$z\sec h\left(\frac{\pi z^2}{h^2}\right)-z\sec h\left(\frac{\pi}{4}\right)\left[1-\frac{\pi}{2}\tanh\left(\frac{\pi}{4}\right)\right]$	[25]	**H-3**
22	$\frac{\cosh\left(\frac{\pi}{2}\right)}{\left[\cosh\left(\frac{\pi}{2}\right)-1\right]}z-\frac{\left(\frac{h}{\pi}\right)\sinh\left(\frac{\pi z}{h}\right)}{\left[\cosh\left(\frac{\pi}{2}\right)-1\right]}$	[80]	**H-4**
23	$\sinh^{-1}\left(\frac{rz}{h}\right)-z\frac{2r}{h\sqrt{r^2+4}}$ $r=3$	[18]	**H-5**
24	$\sinh^{-1}\left[\sin\left(\frac{\pi z}{h}\right)\right]$	[76]	**H-6**
25	$\tanh\left(\frac{rz}{h}\right)-\frac{rz}{h}\sec h^2\frac{r}{2}$ $r=3$	[81]	**H-7**
26	$ze^{-2\left(z/h\right)^2}$	[82]	**E-1**

27	$z\times 3^{\frac{-2}{\log 3}\left(\frac{z}{h}\right)^2}$	[29]	**E-2**
28	$z2.85^{-2(z/h)^2}+0.028z$	[30]	**E-3**
29	$\sin\left(\frac{\pi z}{h}\right)\times e^{\frac{1}{2}\cos\left(\frac{\pi z}{h}\right)}+\frac{\pi z}{2h}$	[30]	**E-4**
30	$\left(\frac{z}{h}\right)^2 m\log\left[e^{z/h}\right]-\frac{m^2 z}{h}\left\{\log\left[e^{1/2}\right]+\frac{1}{4}\right\}$ $m=1.04$	[31]	**L-1**
31	$f(z)=\frac{1}{2}\ln\frac{h-z}{h+z}+\frac{4z}{3h}$	[83]	**L-2**
32	$z\ln\left(1+\frac{4z^2}{h^2}\right)-z\ln 2-z$	[84]	**L-3**

2.2 Strain-displacement relation

Using the linear strain equation, the condition of strain at a given position is expressed by the equation:[85, 86]

$$\varepsilon=\begin{Bmatrix}\frac{\partial u}{\partial x}\\ \frac{\partial v}{\partial y}\\ \frac{\partial u}{\partial y}+\frac{\partial v}{\partial x}\\ \frac{\partial v}{\partial z}+\frac{\partial w}{\partial y}\\ \frac{\partial u}{\partial z}+\frac{\partial w}{\partial x}\end{Bmatrix}=\varepsilon_l \tag{2}$$

The linear strain vector may be expressed by replacing the updated displacement formula from Eq. (2) in Eq. (3).

$$\varepsilon_l=\begin{Bmatrix}\varepsilon_{lb}\\ \varepsilon_{ls}\end{Bmatrix}=\begin{Bmatrix}Z_{lb}\hat{\varepsilon}_{lb}\\ Z_{ls}\hat{\varepsilon}_{ls}\end{Bmatrix} \tag{3}$$

The following matrix structure is used to express ε_{lb} and ε_{ls}.

$$\varepsilon_{lb}=\left\{\frac{\partial u_0}{\partial x}\quad\frac{\partial v_0}{\partial y}\quad\frac{\partial u_0}{\partial y}+\frac{\partial v_0}{\partial x}\quad\frac{\partial \phi_x}{\partial x}\quad\frac{\partial \phi_y}{\partial y}\quad\frac{\partial \phi_x}{\partial y}+\frac{\partial \phi_y}{\partial x}\quad\frac{\partial \theta_x}{\partial x}\quad\frac{\partial \theta_y}{\partial y}\quad\frac{\partial \theta_x}{\partial y}+\frac{\partial \theta_y}{\partial x}\right\}^T \tag{4}$$

$$Z_{lb}=\begin{bmatrix}1&0&0&z&0&0&f(z)&0&0\\ 0&1&0&0&z&0&0&f(z)&0\\ 0&0&1&0&0&z&0&0&f(z)\end{bmatrix} \tag{5}$$

$$\varepsilon_{ls} = \left\{ \frac{\partial \omega_0}{\partial y} + \theta_y \quad \frac{\partial \omega_0}{\partial x} + \theta_x \quad \theta_y \quad \theta_x \right\}^T \tag{6}$$

$$Z_{ls} = \begin{bmatrix} 1 & 0 & f'(z) & 0 \\ 0 & 1 & 0 & f'(z) \end{bmatrix} \tag{7}$$

2.3 Stress and strain relation

The constitutive relations for any layer in the global coordinate (x, y) system due to the existence of an elastic symmetry plane of K^{th} layer, are of the form

$$\{\sigma\}_{3x1} = [\bar{Q}]_{3x3} \{\varepsilon\}_{3x1} \text{ and } \{\tau\}_{2x1} = [\bar{Q}]_{2x2} \{\gamma\}_{2x1} \tag{8}$$

Here (σ_{xx}, σ_{yy}, τ_{xy}, τ_{yz}, τ_{xz}) are the stress and ($\varepsilon_{xx}, \varepsilon_{yy}, \gamma_{xy}, \gamma_{yz}, \gamma_{xz}$) are the strain components of the k^{th} layer in global coordinates, and $\bar{Q}_{ij}$ are the converted material constants from local coordinates at θ angle around the z-axis as illustrated in Fig.1. In any classic finite element textbook, the expression of $\bar{Q}_{ij}$ in terms of material constants in a global coordinate system can be obtained.

As a result, the in-plane stress and transverse shear resultants are described this way:

$$\begin{bmatrix} N_{xx} & M_{xx} & P_{xx} & Q_{xx} & R_{xx} & S_{xx} \\ N_{yy} & M_{yy} & P_{yy} & Q_{yy} & R_{yy} & S_{yy} \\ N_{xy} & M_{xy} & P_{xy} & Q_{xy} & R_{xy} & S_{xy} \end{bmatrix} = \int_{-h/2}^{h/2} \begin{Bmatrix} \sigma_{xx} \\ \sigma_{yy} \\ \tau_{xy} \end{Bmatrix} \{1 \quad z \quad f(z) \quad z^2 \quad zf(z) \quad f^2(z)\} dz \tag{9}$$

$$\begin{bmatrix} N_{yz} & M_{yz} & P_{yz} & Q_{yz} & R_{yz} & S_{yz} \\ N_{xz} & M_{xz} & P_{xz} & Q_{xz} & R_{xz} & S_{xz} \end{bmatrix} = \int_{-h/2}^{h/2} \begin{Bmatrix} \tau_{yz} \\ \tau_{xz} \end{Bmatrix} \{1 \quad z \quad f(z) \quad f'(z) \quad zf'(z) \quad f(z)f'(z)\} dz \tag{10}$$

2.4 Variational Principle

The governing differential equation for the static behaviour of composite laminate is obtained by the principle of virtual work for a given system, using the total Lagrangian approach, is given as:

$$\int_V \left[\delta \{\varepsilon\}^T \{\sigma\} + \delta \left(\frac{\partial w_0}{\partial x} + \phi_x \right)^T \gamma \left(\frac{\partial w_0}{\partial x} + \phi_x \right) + \delta \left(\frac{\partial w_0}{\partial y} + \phi_y \right)^T \gamma \left(\frac{\partial w_0}{\partial y} + \phi_y \right) \right] dV = \int_A \delta w^T P dA \tag{11}$$

The virtual strain energy is represented by the first term in Eq. (12) and is expressed in an alternative manner as:

$$\delta U = \int_V \left(\delta \varepsilon^T \right) \sigma dz dA = \int_V \left(\delta \varepsilon_l \right)^T \bar{Q} \left(\varepsilon_l \right) dz dA \tag{12}$$

$$\delta U = \int_V \left\{ \left(\delta \hat{\varepsilon}_l \right)^T Z_l^T \bar{Q} Z_l \hat{\varepsilon}_l \right\} dz dA \tag{13}$$

The strain energy owing to artificial constraints is represented by the second and third terms in Eq. (12), and the overall formulation is

$$\delta U_{\gamma}=\int_{V}\gamma\left[\delta\left(\frac{\partial w_0}{\partial x}+\phi_x\right)^{T}\left(\frac{\partial w_0}{\partial x}+\phi_x\right)+\delta\left(\frac{\partial w_0}{\partial y}+\phi_y\right)^{T}\left(\frac{\partial w_0}{\partial y}+\phi_y\right)\right]dzdA \tag{14}$$

The virtual work done by the transverse mechanical load is represented by the final term of Eq. (10) and is stated as

$$\delta W_{ext}=\int_{A}\delta w_0 P(x,y)\big|_{z=h/2}\,dA \tag{15}$$

The transverse load applied to the top surface spatially distributed (z=h/2) is represented by $P(x,y)\big|_{z=h/2}$ The external load being treated as a non-follower load for simplicity's sake. It will not vary when the plate deforms.

3. FEM analysis

In finite element method, a nine-nodded isoparametric element with seven degrees of freedom (DOF) per node is formed as shown in Figure 2.

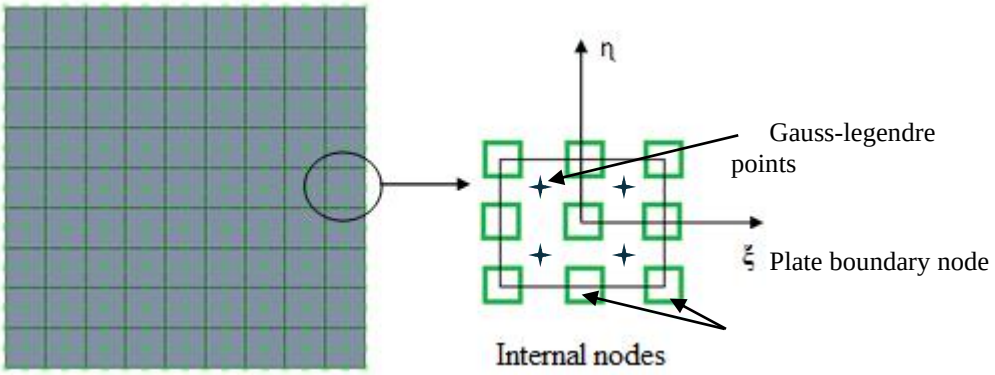

Fig 2. Nine-nodded Q9 Lagrange isoparametric finite element

The laminate domain must be discretized into elements in the finite element (FE) approach. A nine-noded isoparametric element is chosen for its ability to accurately represent complex geometries and displacement fields. The element has nodes at the corners, midpoints of edges, and the center. Lagrangian quadrilateral isoparametric element are used to interpolate the geometry and field variables within the element. These shape functions ensure continuity and smoothness of the displacement field across elements. The continuum displacement vector within the element is discretized at any position such that.

$$\begin{Bmatrix}x\\y\end{Bmatrix}=\sum_{i=1}^{9}N_i\begin{Bmatrix}x_i\\y_i\end{Bmatrix};\ \{u\}=\sum_{i=1}^{9}[I_7]N_i\{q_i\} \tag{16}$$

Where $[I_7]$ is the unit matrix of order seven and $\{q_i\}$ is the vector of nodal field variables at i^{th} node, i.e.

$$\{q_i\}=\{u_{0i}\quad v_{0i}\quad w_{0i}\quad \phi_{xi}\quad \phi_{yi}\quad \theta_{xi}\quad \theta_{yi}\}^{T} \tag{17}$$

The following are the shape function formulas for the nine nodes illustrated in Fig.2:

$$N_1=\frac{1}{4}\xi\eta(\xi-1)(\eta-1); \tag{18}$$

$$N_2=-\frac{1}{2}\xi(\xi-1)(\eta^2-1)\ N_3=\frac{1}{4}\xi\eta(\xi-1)(\eta+1);$$

$$N_4 = -\frac{1}{2}\left(\xi^2 - 1\right)\left(\eta - 1\right)\eta$$

$$N_5 = \left(\xi^2 - 1\right)\left(\eta^2 - 1\right);$$

$$N_6 = -\frac{1}{2}\left(\xi^2 - 1\right)\eta\left(\eta + 1\right)\ N_7 = \frac{1}{4}\xi\left(\xi + 1\right)\eta\left(\eta - 1\right);$$

$$N_8 = -\frac{1}{2}\xi\left(\xi + 1\right)\left(\eta^2 - 1\right) \qquad N_9 = \frac{1}{4}\xi\left(\xi + 1\right)\eta\left(\eta + 1\right)$$

Appendix A contains the complete formula for the linear strain component. Bending and shear stresses may now be expressed in nodal degrees of freedom using Eqs. (5) and (7), as follows

$$\hat{\varepsilon}_{lb} = \sum_{i=1}^{9} B_{bi}^{L} q_i = B_b^L q\,; \qquad \hat{\varepsilon}_{ls} = \sum_{i=1}^{9} B_{si}^{L} q_i = B_s^L q \tag{19}$$

$$\text{Here } q = \left\{ q_1^T q_2^T \cdots q_8^T q_9^T \right\}^T$$

As a result, terms in the explicit expressions of B_b^L and B_s^L need the first Cartesian derivative of the shape function $\left(\frac{\partial N_i}{\partial x}\right)$. The following connection may be used to determine the first derivative of N_i (in Cartesian coordinate) in terms of derivative with respect to parametric coordinate (and) using the chain rule:

$$\begin{Bmatrix} \frac{\partial N_i}{\partial x} \\ \frac{\partial N_i}{\partial y} \end{Bmatrix} = \begin{bmatrix} \frac{\partial x}{\partial \xi} & \frac{\partial y}{\partial \xi} \\ \frac{\partial x}{\partial \eta} & \frac{\partial y}{\partial \eta} \end{bmatrix}^{-1} \begin{Bmatrix} \frac{\partial N_i}{\partial \xi} \\ \frac{\partial N_i}{\partial \eta} \end{Bmatrix} \tag{20}$$

Similarly, the strain-displacement matrix for Eq. (15) may be produced, and the virtual strain energy owing to the penalty can be expressed as:

$$\delta U_\gamma = \left(\delta q\right)^T \int_V \left[B_\gamma \right]^T \left[B_\gamma \right] \gamma dz dA \tag{21}$$

3.1 System of equations

The system of equations for flexural analysis under distributed transverse load is produced by substituting Eqs. (17) and (21) into Eqs. (13), (16), and (23), then omitting the virtual displacement vector $\left(\delta q\right)^T$.

$$\left(K_L + \gamma K_\gamma\right) q = F_P \tag{22}$$

$$K_L = \int_V \left(\left(B^L\right)^T Z_l^T \bar{Q} Z_l B^L \right) dz dA\,; \qquad K_\gamma = \int_V \left[B_\gamma \right]^T \left[B_\gamma \right] dz dA \tag{23}$$

Here, F_P can be written in the following form

$$F_P = \int_A \left\{ w \right\} P\left(x, y\right) dA \tag{24}$$

In which,

$$\{w\}\{q\} = \sum_{i=1}^{9} \{w_i\} q_i ; \qquad \{w\} = \{0 \quad 0 \quad N_i \quad 0 \quad 0 \quad 0 \quad 0\} \tag{25}$$

The overall stiffness is obtained once the linear stiffness matrices have been evaluated.

$$K = \gamma K_\gamma + K_L \tag{26}$$

3.2 Stress recovery technique over the surface

Since the invention of the finite element technique, engineers have struggled to determine the best mesh size to achieve the needed precision. The stress-recovery approach [87] that was employed to create a continuous and optimized stress component is simply addressed in this paragraph. To precisely analyse the stresses, the super convergent patch recovery approach was created. The efficiency of the SPR technique is better than that of its counterparts, direct interpolation and continuous least square projection approaches, according to the literature [88] [46]. The SPR method is used exclusively to derive the in-plane distribution of stresses in this investigation. As seen in the 3D elasticity solution [66], accuracy is high while deriving the in-plane distribution of stresses for bending problems. However, because the current finite element model uses a C^0 continuous Lagrange element, only the displacement is determined to be accurate over the plate. But in most practical applications, the precise distribution of stresses is more critical than displacement. A stress-recovery approach must be employed in the later stage to achieve the exact in-plane variation of stresses to provide accurate stresses throughout the plate geometry.

Furthermore, due to HSDT, the variation of transverse stresses τ_{xz} and τ_{yz} along the thickness anticipated by the current finite element approach is accurate. In addition, it is well documented in the literature that by integrating the 3D elasticity equilibrium equations, we can predict the precise transverse stress distribution [89]. Furthermore, the transverse stresses calculated by the constitutive relation using higher-order theory provide a reasonable estimate of transverse stress change with thickness. As a result, no thickness-direction recovery is employed in this investigation. The enhanced stress components are derived using the SPR approach by taking a least square projection of the calculated stress at Gauss-Legendre points on a patch. The term patch refers to a collection of elements with a vertex node in the middle. To begin, a 'patch' is defined as a localized group of elements that surrounds at least one inner node or is near a boundary node. As illustrated in Figs., a patch can comprise more than two elements and be classed as an internal or border patch.

In the finite element approximation in which the shape function N has a complete expansion of order *p*, the enhanced stress field is considered to be a kind of polynomial in which the values of σ^* vary as a polynomial of order (*p – 1)* to provide consistent improvement in stresses across the patch.

The polynomial expansion described in Eq. (29) is used for modeling in this study.

$$\sigma^* = C_0 + \bar{x}C_1 + \bar{y}C_2 + \bar{x}\,\bar{y}C_3 + \bar{x}^2C_4 + \bar{y}^2C_5 + \bar{x}^2\bar{y}C_6 + \bar{x}\,\bar{y}^2C_7 + \bar{x}^2\,\bar{y}^2C_8 \tag{27}$$

$$\sigma^* = M_i C_i = M\,C \tag{28}$$

Here, with the help of $\bar{x} = x_{sa} - x_v$ and $\bar{y} = y_{sa} - y_v$ the unidentified coefficient which is derived for every stress component accounted inside a patch is C_i. Here, x_{sa} and x_v indicates the x-coordinate of sampling and vertex points, respectively.

While the newly developed NEHSDT and the finite element method offer significant improvements in accuracy and stability for the bending analysis of laminated plates, there are several limitations and potential challenges associated with their practical application in engineering problems. The NEHSDT can be mathematically complex, making their implementation in commercial FEM challenging. Engineers may need advanced knowledge of programming and numerical methods to develop custom solutions or modify existing software. While the NEHSDT have shown close agreement with 3D quasic solutions in theoretical studies, extensive validation and verification against experimental data are necessary to ensure their reliability in real-world applications. This process can be time-consuming and resource

intensive.

It's worth noting that any acceptable polynomial function can be chosen based on the number of sample points and unidentified coefficients collected in a patch. As previously indicated, the unidentified polynomial coefficients are calculated by fitting the predicted stresses to a set of sample locations inside the patch in a least square technique.

$$F = \frac{1}{2}\left(\sigma^* - \sigma\right)^T \left(\sigma^* - \sigma\right) d\Omega_c \tag{29}$$

$$\int_{\Omega_c} \frac{\partial F}{\partial C_i} = \int_{\Omega_c} \left(\frac{\partial \sigma^*}{\partial C_i}\right)^T \left(\sigma^* - \sigma\right) d\Omega_c = 0 \tag{30}$$

$$\int_{\Omega_c} M^T M \, d\Omega_c = \int_{\Omega_c} M^T \sigma d\Omega_c \quad \text{or} \quad AC = B \tag{31}$$

$$A = \int_{\Omega_c} M^T M \, d\Omega_c \text{ and } B = \int_{\Omega_c} M^T \sigma d\Omega_c \tag{32}$$

The patch domain is denoted by the symbol Ω_c . The needed stress value at selected nodes (as shown in the fig) may be determined using Eq. (29) after solving for the unknown coefficient C_i for every stress component. Because of the merging of patches in this patch recovery technique, certain nodes may have more than one value, as seen in Fig.2. As a result, plain aggregating is required to obtain a specific stress evaluation over the geometry.

4. Numerical validations: Results and discussion

The Lagrange basis function, which requires C^0 continuity of the field variables, is used in most displacement-based FE models. Approximating the solution for C^1 continuity using the Hermite role has its own set of challenges in terms of finite element code implementation. Artificial field variables must be used to create the finite element model with HSDT (as per Eq. (2)) using the Lagrange element, which reduces the needed continuity to C^0 Present analysis is focused on implementation of new higher order shear deformation theory with the novel parabolic shear deformation function is developed to analyse the bending response of laminated composite plates. The first section deals with convergence study. A validation study is conducted to demonstrate the user-defined MATLAB program's efficacy and accuracy. The deflection and stresses are normalized as:

$$\bar{w}c = \left(\frac{100h^3 E_2}{q_0 a^4}\right) w\left(\frac{a}{2}, \frac{z}{h}, 0\right),\ \bar{\sigma}_{xx} = \frac{h^2}{q_0 a^2}\sigma_{xx}\left(\frac{a}{2}, \frac{a}{2}, \frac{h}{4}\right), \bar{\sigma}_{yy} = \frac{h^2}{q_0 a^2}\sigma_{yy}\left(\frac{a}{2}, \frac{a}{2}, \frac{h}{4}\right)$$

$$\bar{\sigma}_{xy} = \frac{h^2}{q_0 a^2}\sigma_{xy}\left(0, 0, \frac{z}{h}\right),\ \bar{\sigma}_{yz} = \frac{h}{q_0 a}\sigma_{yz}\left(\frac{a}{2}, 0, 0\right),\ \bar{\sigma}_{xz} = \frac{h}{q_0 a}\sigma_{xz}\left(0, \frac{b}{2}, 0\right)$$

4.1 Material properties

Numerous analyses are carried out during present investigation with the material property as.

Material- 1 $E_1 / E_2 = 25, G_{12} / E_2 = G_{13} / E_2 = 0.5, G_{23} / E_2 = 0.2, \upsilon_{12} = 0.25$

4.2 Boundary conditions

During the numerical analysis in present study, the simply supported condition is considered as:

SSSS: $u_0 = w_0 = \theta_x = \phi_x = 0$ at $y = 0, b$ and $v_0 = w_0 = \theta_y = \phi_y = 0$ at $x = 0, a$;

4.3 Convergence study

The problem of convergence, or an asymptotic behaviour of estimates of correctness of an achieved approximation solution as the finite element mesh grows infinitely thick, is a major topic in the theory of the finite element method. For the orthotropic laminated composite plate, the finite element convergence performance under the action of uniformly distributed load (UDL) and sinusoidal loading (SSL) condition for (0/90/90/0) laminate with SSSS1 simply supported loading condition are shown in Figure 3 (a and b). Figure 3 (a) shows the effect of variation of number of elements over normalised deflection and stress variation occurred in composite plate under UDL and Figure 3 (b) for SSL. From the figure it is clear that after 6 number of elements there is no variation in values of deflection and stresses found, and hence can say the values were get converged. So, for further study 6 numbers of element are selected.

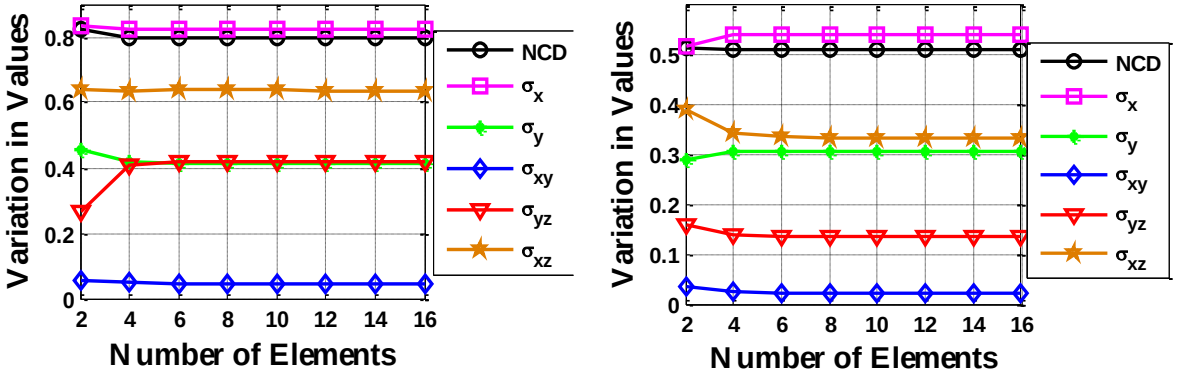

Fig. 3 Convergence study

4.4 Parametric study

Figure 4 shows the effect of novel fuzzy function (r) parameter variation over normalised deflection of the composite plate. For the present investigation plate aspect ratio= 1 and thickness ratio=10 under SSSS boundary condition and shown in Figure 4 also elaborate the nature of bending and shear stress distribution in thickness direction with the variation of novel fuzzy function (r). The 'r' in the NEHSDT is a fudge factor whose value is optimised by an inverse method. A MATLAB code is developed to obtain the results. By using various values of ''r", deflection and stresses in laminated plates is determined, and error between the results of proposed theory and 3D solution in literature was minimized. The presented numerical results are compared with the existing results to illustrate the correctness and robustness of the finite element method. Figure 4 (a) shows with increasing the value of the fuzzy function parameter (r) value of the normalised plate deflection comes nearer to the 3D Quasis solution utilised by Tran and Kim [90] and 2D plate theory by Reddy and Liu [91]. Result shows that normalised deflection, bending and shear stress values are closely validated with the results presented in literature at the value of r = 1.6. Accuracy in the results contributed a lot when it comes into a large scale. If even infinitely improvement come through the theory/numerically implementation, it will serve the scientific community a lot.

Figure 5 shows give an exact parabolic distribution of transverse shear stress over the thickness with the utilisation of novel parabolic shear deformation function. Result evaluated with the variation of fuzzy function parameter (r), and it is noticed that though r parameter is get varied, the parabolic nature of the shear stress distribution in thickness direction (*z/h*) does not violated. The shear stress distribution is maximum at the centre and zero at the end of the plate extreme surface which shows the uniformity of the plate. The present study intended to focus on the integrity of the new higher order shear deformation theory towards Parabolic shear deformation function satisfied all the necessary conditions required for the transverse shear function. The present NEHSDT approximately parabolic transverse shear deformation distribution and also displacement field satisfies the traction free boundary conditions at top and bottom surface of the plate and hence the requirement of shear correction factor vanishes. Hence, we have just satisfied all the necessary conditions for the development of a new transverse shear functions suitable for the analysis of laminated plate and by implementing it is notice that NEHSDT give the better results as compared to other functions in literature.

The effect of algebraic, trigonometric, inverse trigonometric, logarithmic, exponential, hyperbolic functionalised plate theory over normalised plate deflection shown in Figure 6 (a, b) and Table 2 for stress variation along X, Y, XY and YZ direction. To evaluate the result from algebraic, trigonometric, inverse trigonometric, logarithmic, exponential, hyperbolic theories the function is utilised from literatures mentioned in Tables 1 and further compared these results

with newly developed HSDT.

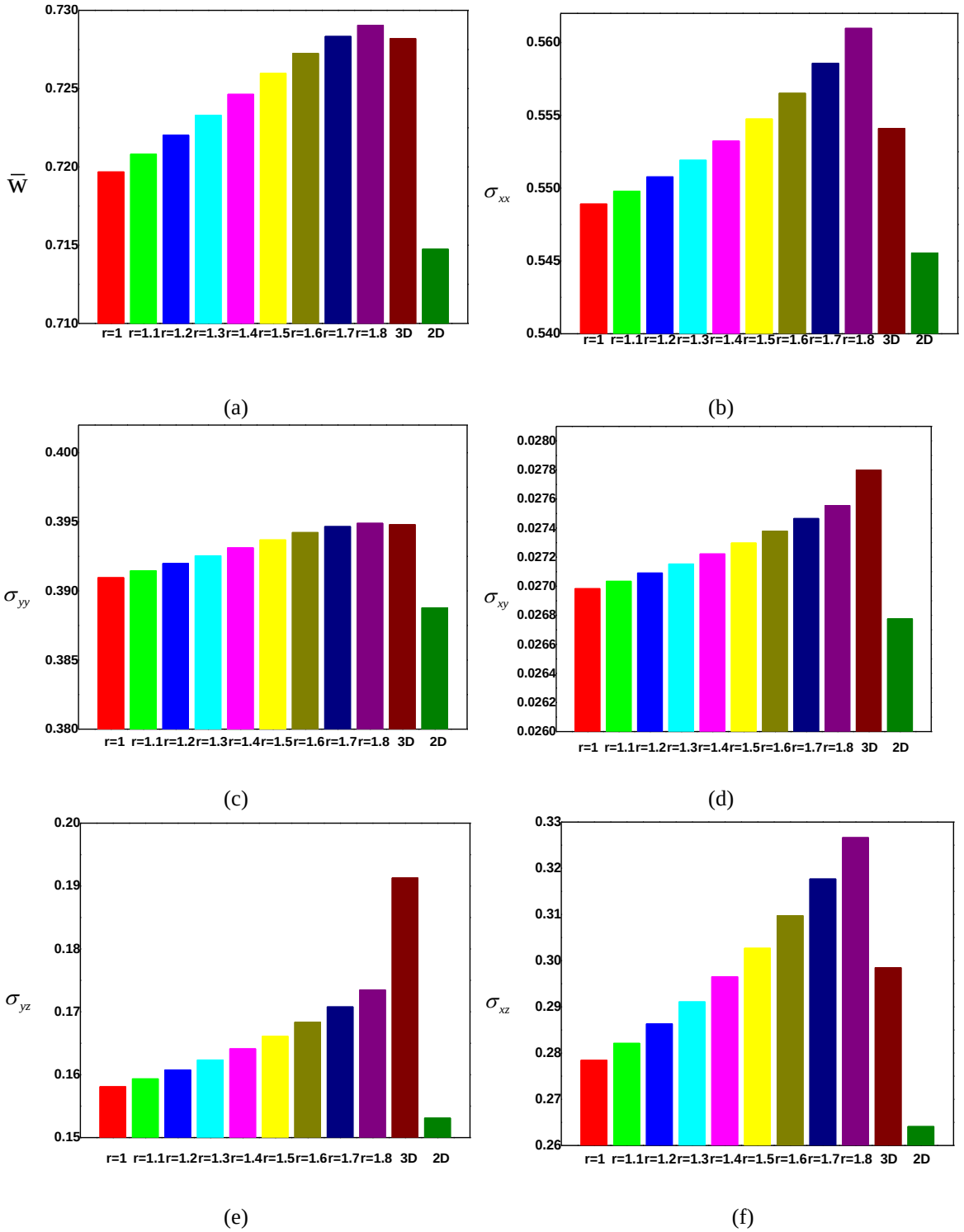

Fig. 4 Effect of fuzzy function (r) variation over (a) normalised deflection (b) σ_{xx} (c) σ_{yy} (d) σ_{xy} (e) σ_{yz} (f) σ_{xz}

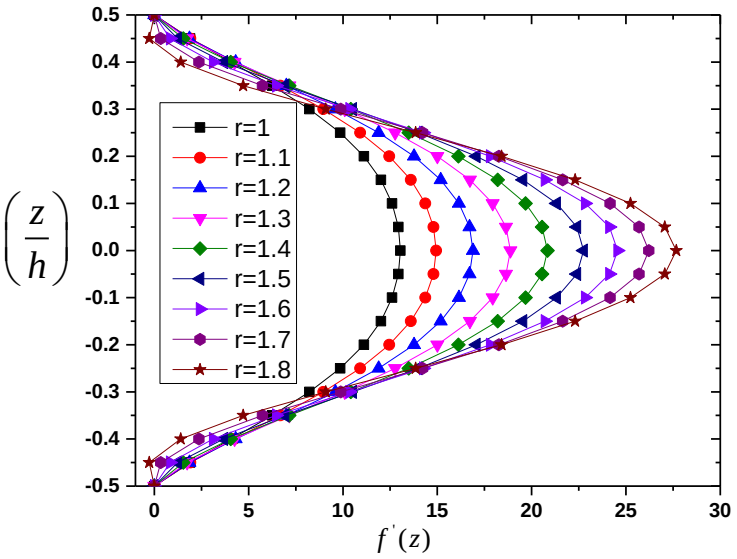

Fig. 5 Exact parabolic distribution of transverse shear stress over the thickness direction

For the present analysis four layered cross ply composite laminate of orientation (0/90/90/0) with span to plate thickness ratio = 10 under simply supported boundary condition were used. Figure 6 also define the nature of variation for normalised central deflection between above mentioned theories and newly developed HSDT with parabolic shear deformation function during validation with 3D elastic means 3D Quasis result reported by Tran and Kim [90] results. For the present investigation simply supported laminated composite plate (0/90/90/0) with plate thickness ratio 10 is assumed. It is clearly observed that there is wide variation observed between algebraic, trigonometric, inverse trigonometric, logarithmic, exponential, hyperbolic functionalised plate theory evaluated on deflection and also compared with 3D Quasis result in the literature results. But the amount of deviation is goes on decreasing with the implementation of new HSDT with increment fuzzy parameter (r), and it is closely validated at the value of r=1.6.

As we are aware that along with the uniformly distributed load it is always mandatory to study the effect of another type of loading over structural element. So, in further study sinusoidal loading is applied over the laminated composite plate. Figure 7 shows the comparison of different functional theories and presently utilised new HSDT with Quasis 3D [90] result for normalised central deflection occurs in composite plate. For the analysis laminated composite plate with ply orientation of (0/90/0), plate thickness ratio of 10 is used. Orthotropic material properties of the composite plate are, $E_1 = 25E_2, \upsilon_{12} = 0.25, G_{12} = 0.5E_2, G_{23} = 0.2E_2, \upsilon_{21} = (E_2/E_1)\upsilon_{12}$. The effectiveness of the presently implemented novel parabolic shear deformation theory shows close agreement of normalised central deflection with the Quasis 3D [90][90] theory, than any other functional theories.

Along with the deflection validation for the effective structural analysis it is mandatory to analyse the stress variation in composite plate along x, y and through thickness direction manes xz. So, in figures 8, 9, and 10 the stress variation along x, y and xz direction are given. As shown in Figure 8, the percentage deviation observed in algebraic functionalised theory from Quasis 3D are 1.4835, 1.4835, 1.4835, 1.4835, 0.5206, 3.8021 for A1, A2, A3, A4, A5, A6 respectively. The deviation of trigonometric functionalised theory result from Quasis 3D one are 0.9289, 0.9289, 1.6697, 1.4835, 0.3417, and 5.3422 for T1 to T6. Similarly in case of inverse trigonometric functionalised theory percentage deviation from Quasis 3D theory are 1.4835, 1.0536, 0.3417, 0.8766, 0.1989, and 0.1989 for IT1 to IT6. The deviations of logarithmic functionalised theory result from Quasis 3D one are 2.04, 2.42, and 0.326 for L1 to L3. The deviation of hyperbolic functionalised theory result from Quasis 3D one are 1.67, 1.11, 2.61, 2.04, 0.699, 0.342 for H1 to H6, and for exponential theory the percentage deviation are 0.38, 0.38, 0.38 for E1 to E3. But whenever observing the percentage deviation between Quasis 3D and presently used HSDT, it is 0.0721%, which is lowest among all the functional theories.

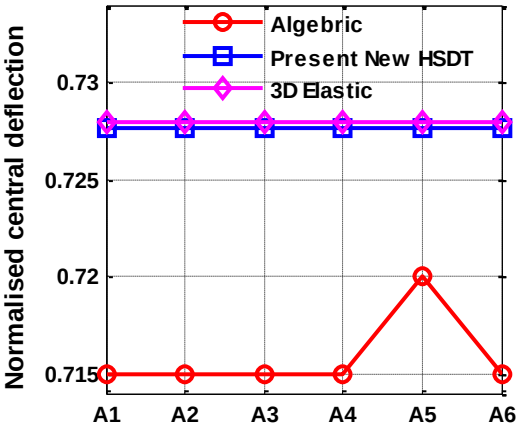

(a)

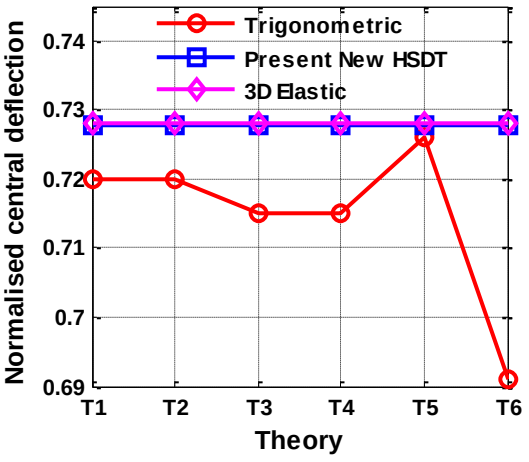

(b)

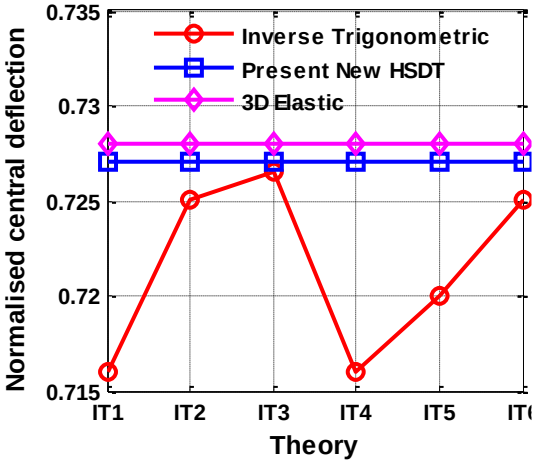

(c)

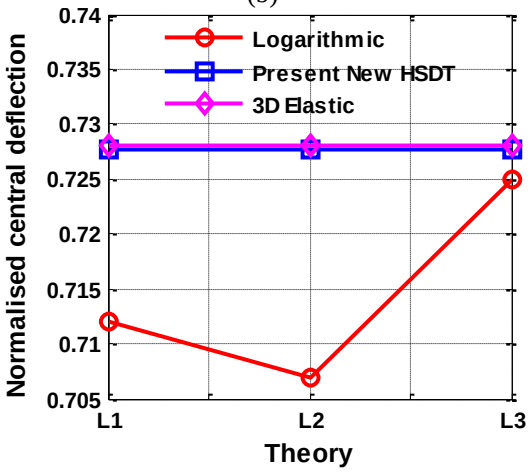

(d)

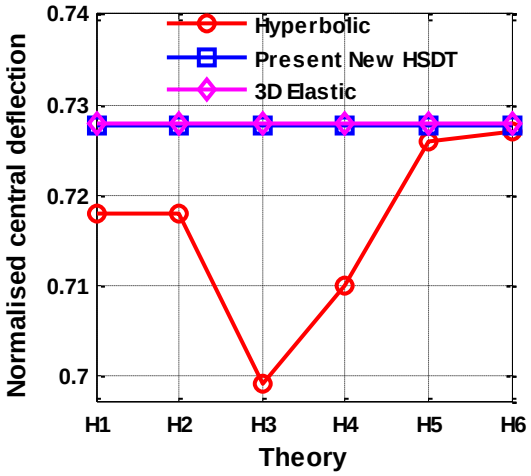

(e)

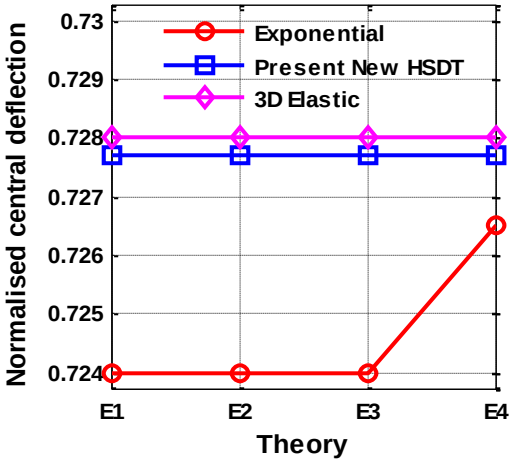

(f)

Fig. 6 Effect of various functions used in theories over normalised central deflection

Table 2 Evaluation of deflection and stresses utilising various theories.

Theory		NCD	σ_x	σ_y	τ_{xz}	τ_{yz}
Quasis 3D [90]		0.7282	0.5541	0.3918	0.1913	0.2985
Present	**r=1.6**	0.7270	0.5570	0.3940	0.1680	0.3100
Algebraic	**A-1**	0.715	0.546	0.389	0.153	0.264
	A-2	0.715	0.546	0.389	0.153	0.264
	A-3	0.715	0.546	0.389	0.153	0.264
	A-4	0.715	0.546	0.389	0.153	0.264
	A-5	0.727	0.557	0.394	0.168	0.311
	A-6	0.72	0.576	0.39	0.165	0.365
	A-7	0.715	0.546	0.389	0.153	0.264
Trigonometric	**T-1**	0.72	0.549	0.391	0.158	0.279
	T-2	0.72	0.549	0.391	0.158	0.279
	T-3	0.715	0.545	0.389	0.153	0.264
	T-4	0.715	0.546	0.389	0.153	0.264
	T-5	0.727	0.556	0.384	0.168	0.309
	T-6	0.691	0.526	0.378	0.141	0.226
Inverse Trigonometric	**IT-1**	0.716	0.546	0.389	0.154	0.267
	IT-2	0.718	0.56	0.394	0.176	0.354
	IT-3	0.727	0.556	0.394	0.163	0.313
	IT-4	0.726	0.559	0.395	0.177	0.333
	IT-5	0.725	0.553	0.393	0.164	0.307
	IT-6	0.725	0.553	0.393	0.164	0.307
Hyperbolic	**H-1**	0.718	0.545	0.39	0.154	0.265
	H-2	0.718	0.548	0.39	0.157	0.275
	H-3	0.699	0.54	0.382	0.136	0.222
	H-4	0.71	0.543	0.387	0.149	0.252
	H-5	0.718	0.558	0.395	0.176	0.329
	H-6	0.727	0.556	0.394	0.164	0.319
	H-7	0.729	0.561	0.395	0.18	0.343
Exponential Exponential	**E-1**	0.724	0.552	0.393	0.163	0.294
	E-2	0.724	0.552	0.393	0.163	0.294
	E-3	0.724	0.552	0.393	0.163	0.294
	E-4	0.729	0.561	0.395	0.177	0.335
Logarithmic Logarithmic	**L-1**	0.712	0.543	0.388	0.152	0.259
	L-2	0.707	0.541	0.386	0.147	0.246
	L-3	0.722	0.5523	0.393	0.167	0.313

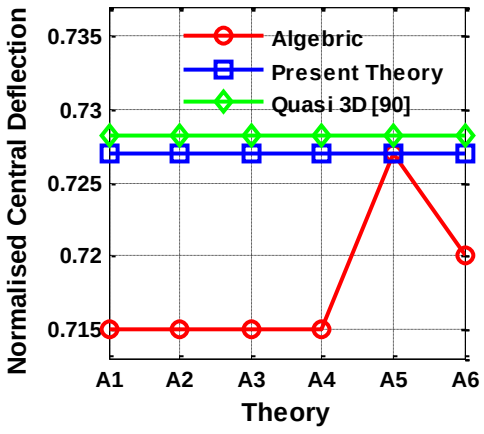

(a)

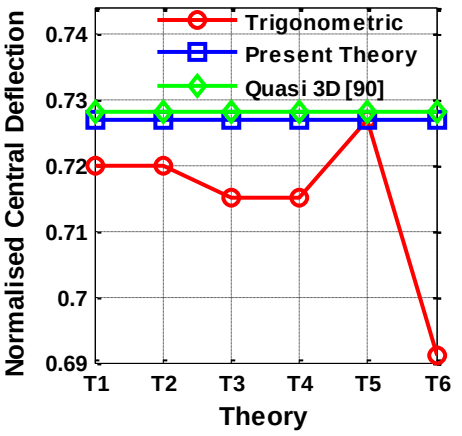

(b)

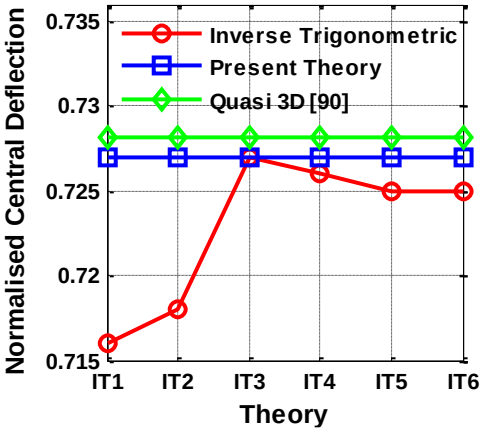

(c)

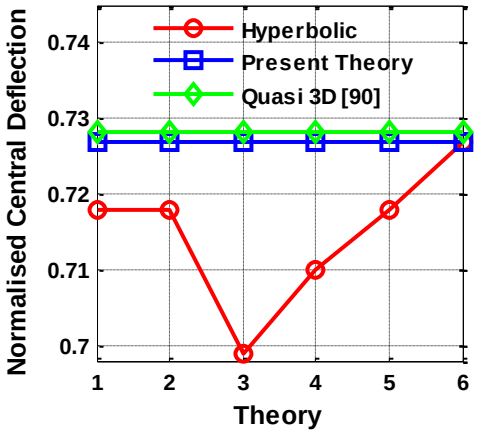

(d)

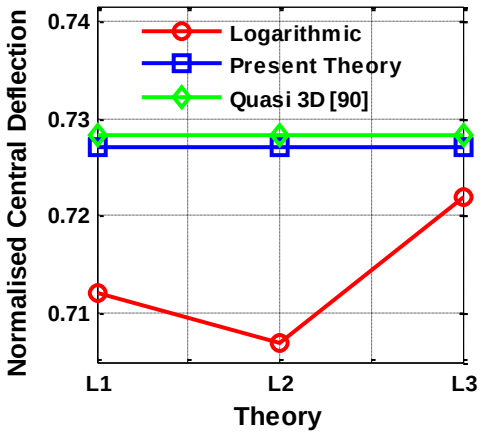

(e)

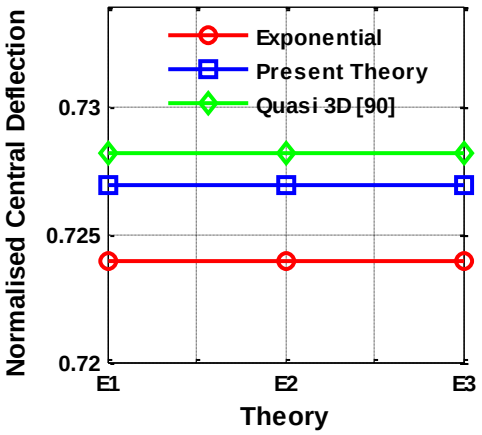

(f)

Fig. 7 Comparison of different function utilised in present new HSDT with Quasis 3D [90][90] result for normalised central deflection

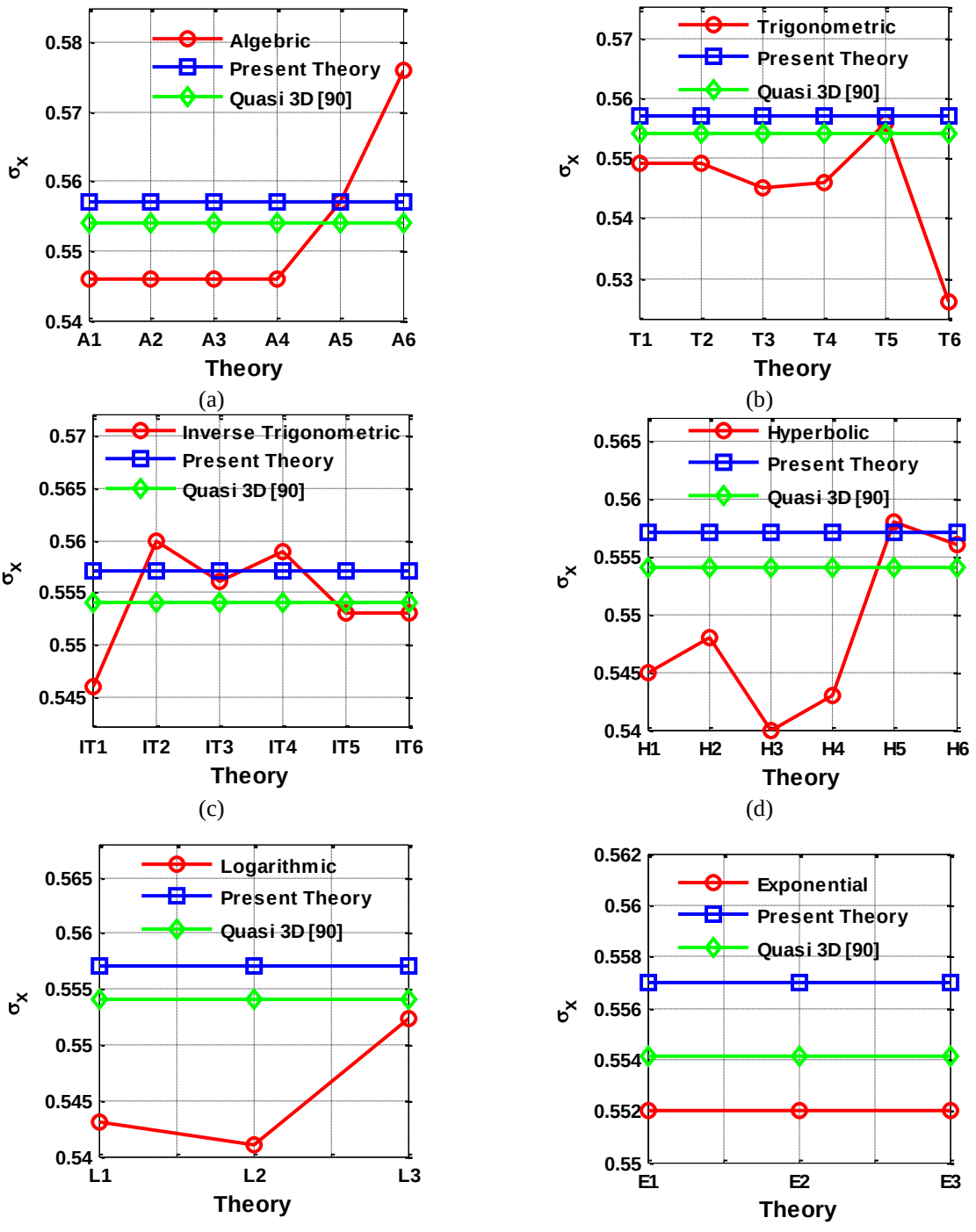

Fig. 8 Comparison of different function utilised in present new HSDT with Quasis 3D [90] result for normal stress in X-direction

Similarly in Figure 9, the percentage deviation in σ_y observed with the use of algebraic functionalised theory from Quasis 3D [90] are 0.7197, 0.7197, 0.7197, 0.7197, 0.5584, 0.4615 for A1 to A6 respectively. The deviation of trigonometric functionalised theory result from 3D elastic one are 0.2046, 0.2046, 0.7197, 0.7197, 2.0312, 3.6507 for T1 to T6. Similarly in case of inverse trigonometric functionalised theory percentage deviation from Quasis 3D [90] theory are 0.7197, 0.5584, 0.5584, 0.8101, 0.3053, and 0.3053 for IT1 to IT6. The deviations of logarithmic functionalised theory result from 3D elastic one are 0.9793, 1.5025, and 0.3053 for L1 to L3. The deviation of hyperbolic functionalised theory result from Quasis 3D [90] one are 0.46154, 0.46154, 2.56545, 1.2403, 0.8101, 0.5584 for H1 to

H6, and for exponential theory the percentage deviation are 0.3053, 0.3053, 0.3053, 0.8101 for E1 to E4. Whenever observing the percentage deviation between Quasis 3D [90] and presently used HSDT, it is 0.1022%, which is lowest among all the functional theories.

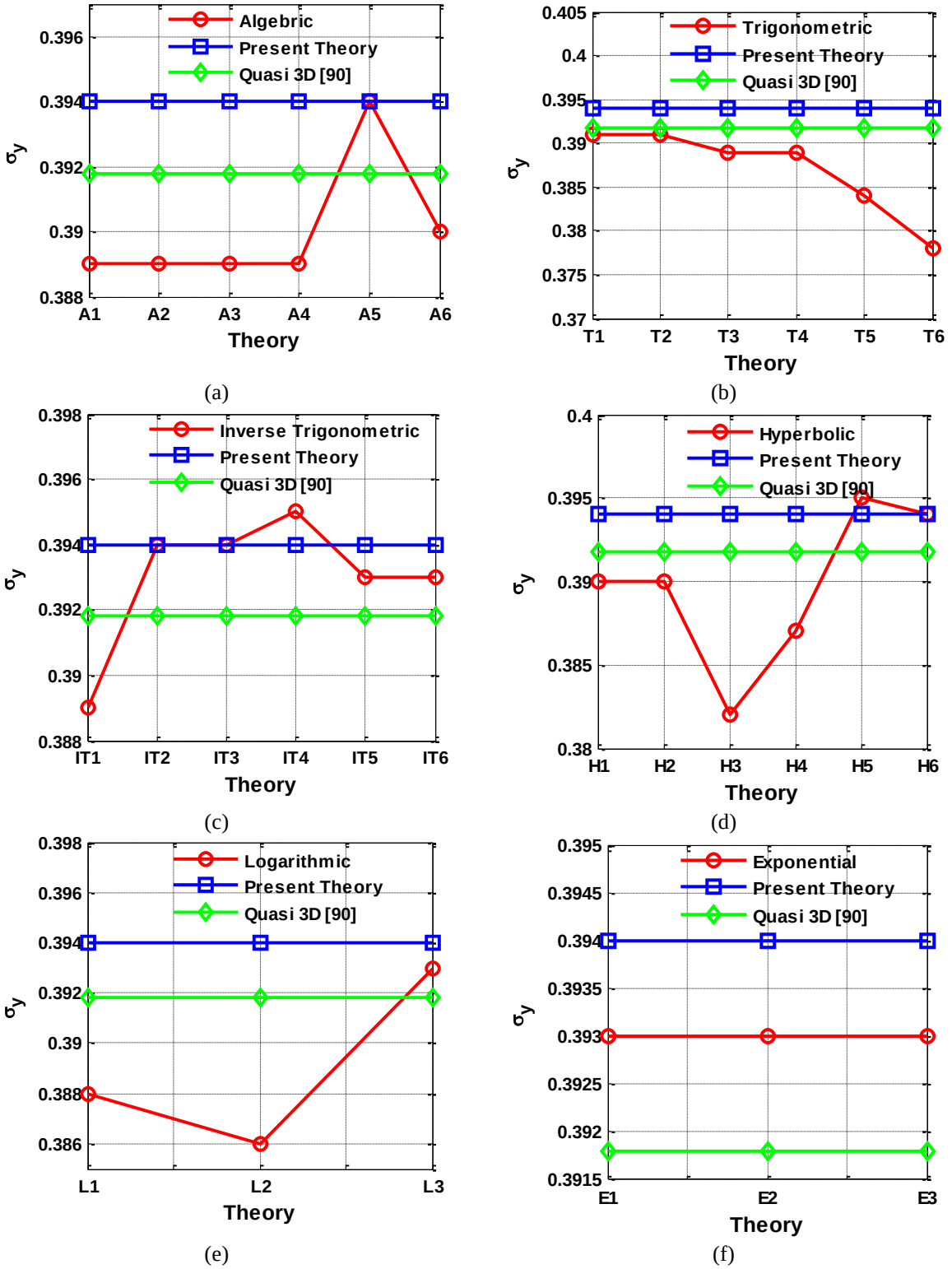

Fig. 9 Comparison of different function utilised in present new HSDT with Quasis 3D [90] result for normal stress in Y-direction

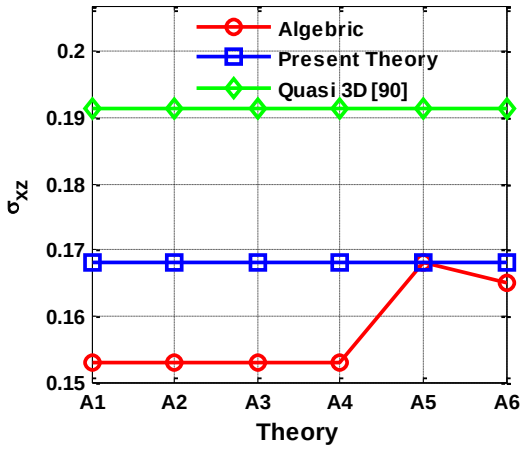

(a)

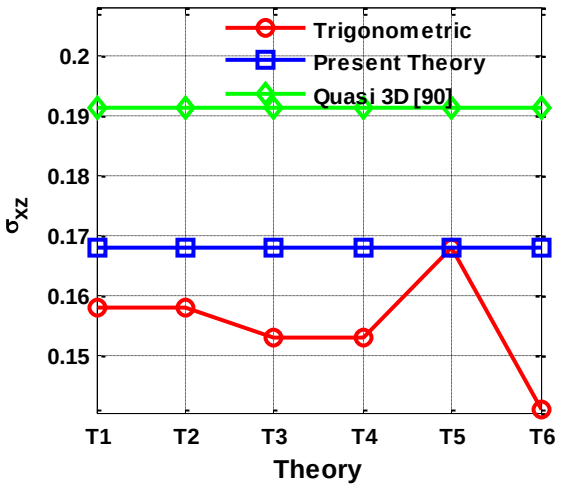

(b)

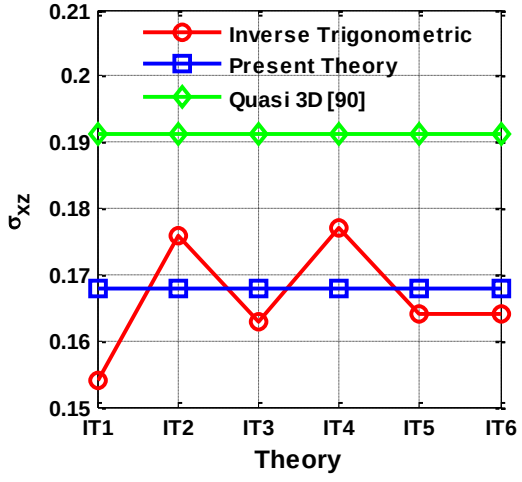

(c)

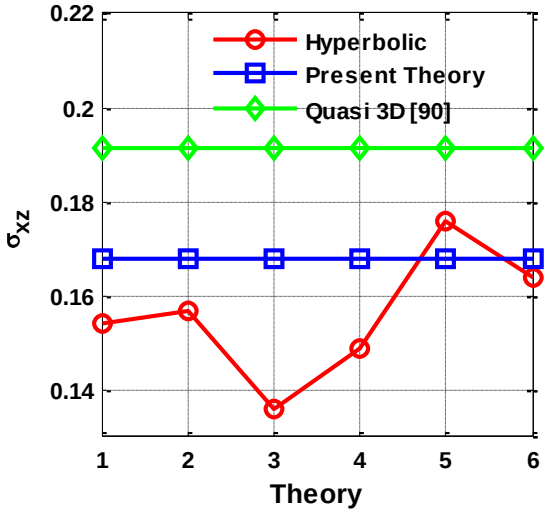

(d)

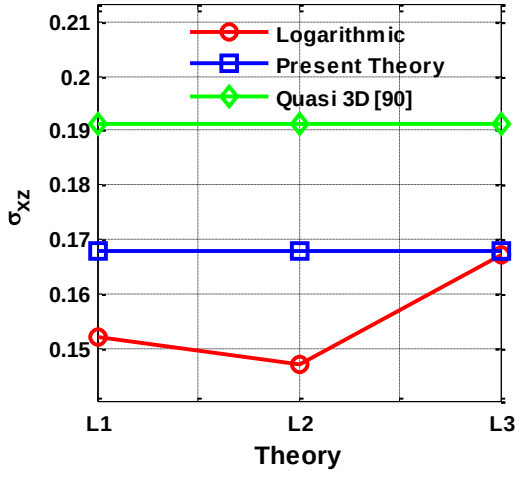

(e)

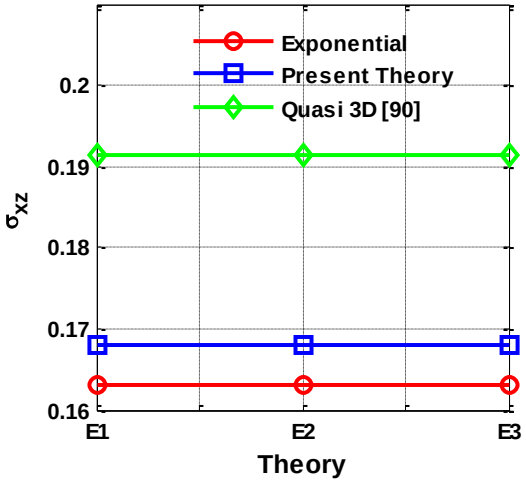

(f)

Fig. 10 Comparison of different function utilised in present new HSDT with Quasis 3D [90] result for normal stress in XZ-direction

In a deflection and stress analysis it is necessary to evaluate the through thickness distribution of the stresses. Figure 10 shows the nature of variation as well as comparison of the shear stress with Quasis 3D [90] theory and

presently implemented parabolic HSDT. From the figure it is clear that as compared to any other functional theory, the percentage deviation between novel parabolic shear deformation theory and Quasis 3D [90] theory is lowest which 3.4054% is. The average percentage deviation of algebraic, trigonometric, inverse trigonometric, logarithmic, hyperbolic, exponential from Quasis 3D [90] theory is 21.656%, 23.626%, 15.274%, 23.514%, 23.41% and 15.041% respectively. So, from Figures 8, 9, 10 it clearly understood the efficiency and effectiveness of the novel parabolic shear deformation theory.

Conclusions:

Present study is focused on new higher-order shear deformation theory (HSDT) to examine the flexural analysis of multi-layered laminated symmetric and non-symmetric composite plates. The present theory gives an exact parabolic distribution of transverse shear stress over the thickness and fulfils the traction-free boundary conditions on the outer surfaces of multi-layered laminated plates. The governing equations are solved using the finite element method. In this finite element method, a nine-nodded isoparametric element with seven degrees of freedom per node is formed especially for this purpose. Following conclusions are summarised from the study,

1. Convergence and validation study shows the effectiveness and accuracy of the presently utilized model and method of investigation.
2. The study is focused on justifying the effective implementation of new higher-order shear deformation theory (HSDT) with fuzzy parameter (r).
3. It is clearly observed that there is wide variation observed between algebraic, Trigonometric, Inverse trigonometric, Logarithmic, Exponential, and Hyperbolic functionalised plate theory evaluated deflection and 3D elastic literature results. But the amount of deviation goes on decreasing with the implementation of new HSDT with fuzzy increment parameter (r), and it is closely validated at the value of r=1.6.

According to this study, the current model accurately predicts the bending analyses of the laminated composite plate. It follows that the proposed computational method can be used to analyze the bending of thin and thick laminated plates with various fiber orientations. Future research can build on new HSDT model by incorporating additional complexities, such as dynamic loading conditions, multi-scale modeling, and non-linear material behavior. This will further enhance the accuracy and applicability of laminated composite plate analyses. The present theory may also extend to panel and shells problems

References

[1] J. M. Whitney, 1987, *Structural Analysis of Laminated Anisotropic Plates*, CRC Press,

[2] R. Kumar, A. Lal, B. N. Singh, J. Singh, Numerical simulation of the thermomechanical buckling analysis of bidirectional porous functionally graded plate using collocation meshfree method, *Proceedings of the Institution of Mechanical Engineers, Part L: Journal of Materials: Design and Applications*, Vol. 236, No. 4, pp. 787-807, 2022.

[3] S. Khare, N. D. Mittal, Axisymmetric bending and free vibration of symmetrically laminated circular and annular plates having elastic edge constraints, *Ain Shams Engineering Journal*, Vol. 10, No. 2, pp. 343-352, 2019.

[4] S. Khare, N. D. Mittal, Free vibration of thick laminated circular and annular plates using three-dimensional finite element analysis, *Alexandria Engineering Journal*, Vol. 57, No. 3, pp. 1217-1228, 2018.

[5] A. K. Noor, W. S. Burton, Assessment of shear deformation theories for multilayered composite plates, 1989.

[6] J. Reddy, D. Robbins Jr, Theories and computational models for composite laminates, 1994.

[7] D. Li, Layerwise theories of laminated composite structures and their applications: a review, *Archives of Computational Methods in Engineering*, Vol. 28, pp. 577-600, 2021.

[8] A. Gupta, A. Ghosh, Isogeometric static and dynamic analysis of laminated and sandwich composite plates using nonpolynomial shear deformation theory, *Composites Part B: Engineering*, Vol. 176, pp. 107295, 2019.
[9] E. Reissner, The effect of transverse shear deformation on the bending of elastic plates, 1945.
[10] R. Mindlin, Influence of rotatory inertia and shear on flexural motions of isotropic, elastic plates, 1951.
[11] A. S. Sayyad, Y. M. Ghugal, On the free vibration analysis of laminated composite and sandwich plates: A review of recent literature with some numerical results, *Composite structures*, Vol. 129, pp. 177-201, 2015.
[12] Z. Wu, R. Chen, W. Chen, Refined laminated composite plate element based on global–local higher-order shear deformation theory, *Composite structures*, Vol. 70, No. 2, pp. 135-152, 2005.
[13] M. Aydogdu, Comparison of various shear deformation theories for bending, buckling, and vibration of rectangular symmetric cross-ply plate with simply supported edges, *Journal of Composite materials*, Vol. 40, No. 23, pp. 2143-2155, 2006.
[14] A. Idlbi, M. Karama, M. Touratier, Comparison of various laminated plate theories, *Composite Structures*, Vol. 37, No. 2, pp. 173-184, 1997.
[15] M. Levy, Memoire sur la theorie des plaques elastiques planes, *Journal de mathématiques pures et appliquées*, Vol. 3, pp. 219-306, 1877.
[16] J. Monge, J. Mantari, Best non-polynomial shear deformation theories for cross-ply single skin and sandwich shells, *Engineering Structures*, Vol. 203, pp. 109678, 2020.
[17] B. R. Thakur, S. Verma, B. Singh, D. Maiti, Dynamic analysis of folded laminated composite plate using nonpolynomial shear deformation theory, *Aerospace Science and Technology*, Vol. 106, pp. 106083, 2020.
[18] N. Grover, D. Maiti, B. Singh, A new inverse hyperbolic shear deformation theory for static and buckling analysis of laminated composite and sandwich plates, *Composite Structures*, Vol. 95, pp. 667-675, 2013.
[19] T. N. Nguyen, C. H. Thai, H. Nguyen-Xuan, On the general framework of high order shear deformation theories for laminated composite plate structures: A novel unified approach, *International Journal of Mechanical Sciences*, Vol. 110, pp. 242-255, 2016.
[20] A. M. Zenkour, Generalized shear deformation theory for bending analysis of functionally graded plates, *Applied Mathematical Modelling*, Vol. 30, No. 1, pp. 67-84, 2006.
[21] J. Mantari, A. Oktem, C. G. Soares, A new trigonometric shear deformation theory for isotropic, laminated composite and sandwich plates, *International Journal of Solids and Structures*, Vol. 49, No. 1, pp. 43-53, 2012.
[22] N. Grover, B. Singh, D. Maiti, New nonpolynomial shear-deformation theories for structural behavior of laminated-composite and sandwich plates, *AIAA journal*, Vol. 51, No. 8, pp. 1861-1871, 2013.
[23] K. Soldatos, A transverse shear deformation theory for homogeneous monoclinic plates, *Acta Mechanica*, Vol. 94, No. 3, pp. 195-220, 1992.
[24] N. El Meiche, A. Tounsi, N. Ziane, I. Mechab, A new hyperbolic shear deformation theory for buckling and vibration of functionally graded sandwich plate, *International Journal of Mechanical Sciences*, Vol. 53, No. 4, pp. 237-247, 2011.
[25] S. Akavci, A. Tanrikulu, Buckling and free vibration analyses of laminated composite plates by using two new hyperbolic shear-deformation theories, *Mechanics of Composite Materials*, Vol. 44, pp. 145-154, 2008.
[26] R. Kumar, A. Lal, B. Singh, J. Singh, Meshfree approach on buckling and free vibration analysis of porous FGM plate with proposed IHHSDT resting on the foundation, *Curved and Layered Structures*, Vol. 6, No. 1, pp. 192-211, 2019.
[27] R. Kumar, M. Bajaj, J. Singh, K. K. Shukla, New HSDT for free vibration analysis of elastically supported porous bidirectional functionally graded sandwich plate using collocation method, *Proceedings of the Institution of Mechanical Engineers, Part C: Journal of Mechanical Engineering Science*, Vol. 236, No. 16, pp. 9109-9123, 2022.
[28] M. Karama, K. Afaq, S. Mistou, Mechanical behaviour of laminated composite beam by the new multi-layered laminated composite structures model with transverse shear stress continuity, *International Journal of solids and structures*, Vol. 40, No. 6, pp. 1525-1546, 2003.
[29] M. Aydogdu, A new shear deformation theory for laminated composite plates, *Composite structures*, Vol. 89, No. 1, pp. 94-101, 2009.
[30] J. Mantari, A. Oktem, C. G. Soares, Static and dynamic analysis of laminated composite and sandwich plates and shells by using a new higher-order shear deformation theory, *Composite structures*, Vol. 94, No. 1, pp. 37-49, 2011.

[31] S. Sarangan, B. Singh, Higher-order closed-form solution for the analysis of laminated composite and sandwich plates based on new shear deformation theories, *Composite Structures*, Vol. 138, pp. 391-403, 2016.
[32] J. N. Reddy, A simple higher-order theory for laminated composite plates, 1984.
[33] R. Shimpi, H. Patel, A two variable refined plate theory for orthotropic plate analysis, *International Journal of Solids and Structures*, Vol. 43, No. 22-23, pp. 6783-6799, 2006.
[34] S.-E. Kim, H.-T. Thai, J. Lee, Buckling analysis of plates using the two variable refined plate theory, *Thin-Walled Structures*, Vol. 47, No. 4, pp. 455-462, 2009.
[35] J. Mantari, A simple polynomial quasi-3D HSDT with four unknowns to study FGPs. Reddy's HSDT assessment, *Composite Structures*, Vol. 137, pp. 114-120, 2016.
[36] J. Reddy, A review of refined theories of laminated composite plates, *The shock and vibration digest*, Vol. 22, No. 7, pp. 3-17, 1990.
[37] V. Vasil'Ev, Theory of thin plates, *Rossijskaya Akademiya Nauk Izvestiya Mekhanika Tverdogo Tela*, Vol. 3, pp. 26-47, 1992.
[38] E. Carrera, Theories and finite elements for multilayered, anisotropic, composite plates and shells, *Archives of computational methods in engineering*, Vol. 9, pp. 87-140, 2002.
[39] C. Pryor Jr, R. Barker, A finite-element analysis including transverse shear effects for applications to laminated plates, *AIAA journal*, Vol. 9, No. 5, pp. 912-917, 1971.
[40] C. W. Bert, M. Malik, Differential quadrature method in computational mechanics: a review, 1996.
[41] S. C. Panda, R. Natarajan, Finite element analysis of laminated composite plates, *International journal for numerical methods in engineering*, Vol. 14, No. 1, pp. 69-79, 1979.
[42] G. Ramtekkar, Y. Desai, A. Shah, Application of a three-dimensional mixed finite element model to the flexure of sandwich plate, *Computers & structures*, Vol. 81, No. 22-23, pp. 2183-2198, 2003.
[43] O. C. Zienkiewicz, R. L. Taylor, 2000, *The finite element method: solid mechanics*, Butterworth-heinemann,
[44] I. Fried, A. Johnson, A. Tessler, Minimal-degree thin triangular plate and shell bending finite elements of order two and four, *Computer methods in applied mechanics and engineering*, Vol. 56, No. 3, pp. 283-307, 1986.
[45] E. N. Dvorkin, *On nonlinear finite element analysis of shell structures*, Thesis, Massachusetts Institute of Technology, 1984.
[46] S. Verma, B. R. Thakur, B. Singh, D. Maiti, Geometrically nonlinear flexural analysis of multilayered composite plate using polynomial and non-polynomial shear deformation theories, *Aerospace Science and Technology*, Vol. 112, pp. 106635, 2021.
[47] M. Motezaker, R. Kolahchi, D. K. Rajak, S. Mahmoud, Influences of fiber reinforced polymer layer on the dynamic deflection of concrete pipes containing nanoparticle subjected to earthquake load, *Polymer Composites*, Vol. 42, No. 8, pp. 4073-4081, 2021.
[48] R. Kolahchi, B. Keshtegar, N.-T. Trung, Optimization of dynamic properties for laminated multiphase nanocomposite sandwich conical shell in thermal and magnetic conditions, *Journal of Sandwich Structures & Materials*, Vol. 24, No. 1, pp. 643-662, 2022.
[49] M. H. Hajmohammad, A. Farrokhian, R. Kolahchi, Dynamic analysis in beam element of wave-piercing Catamarans undergoing slamming load based on mathematical modelling, *Ocean Engineering*, Vol. 234, pp. 109269, 2021.
[50] M. Al-Furjan, M. H. Hajmohammad, X. Shen, D. K. Rajak, R. Kolahchi, Evaluation of tensile strength and elastic modulus of 7075-T6 aluminum alloy by adding SiC reinforcing particles using vortex casting method, *Journal of Alloys and Compounds*, Vol. 886, pp. 161261, 2021.
[51] M. Al-Furjan, M. Xu, A. Farrokhian, G. S. Jafari, X. Shen, R. Kolahchi, On wave propagation in piezoelectric-auxetic honeycomb-2D-FGM micro-sandwich beams based on modified couple stress and refined zigzag theories, *Waves in Random and Complex Media*, pp. 1-25, 2022.
[52] R. Kumar, B. Singh, J. Singh, Geometrically nonlinear analysis for flexure response of FGM plate under patch load, *Mechanics Based Design of Structures and Machines*, Vol. 51, No. 11, pp. 6532-6556, 2023.
[53] M. Al-Furjan, Y. Yang, A. Farrokhian, X. Shen, R. Kolahchi, D. K. Rajak, Dynamic instability of nanocomposite piezoelectric-leptadenia pyrotechnica rheological elastomer-porous functionally graded materials micro viscoelastic beams at various strain gradient higher-order theories, *Polymer Composites*, Vol. 43, No. 1, pp. 282-298, 2022.
[54] M. Al-Furjan, C. Yin, X. Shen, R. Kolahchi, M. S. Zarei, M. Hajmohammad, Energy absorption and vibration of smart auxetic FG porous curved conical panels resting on the frictional viscoelastic torsional substrate, *Mechanical Systems and Signal Processing*, Vol. 178, pp. 109269, 2022.

[55] M. Al-Furjan, L. Shan, X. Shen, R. Kolahchi, D. K. Rajak, Combination of FEM-DQM for nonlinear mechanics of porous GPL-reinforced sandwich nanoplates based on various theories, *Thin-Walled Structures*, Vol. 178, pp. 109495, 2022.

[56] R. Kumar, B. Singh, J. Singh, J. Singh, Meshfree approach for flexure analysis of bidirectional porous FG plate subjected to I, L, and T types of transverse loading, *Aerospace Science and Technology*, Vol. 129, pp. 107824, 2022.

[57] C. Chu, L. Shan, M. Al-Furjan, M. Zarei, M. Hajmohammad, R. Kolahchi, Experimental study for the effect of hole notched in fracture mechanics of GLARE and GFRP composites subjected to quasi-static loading, *Theoretical and Applied Fracture Mechanics*, Vol. 122, pp. 103624, 2022.

[58] M. Al-Furjan, R. Kolahchi, L. Shan, M. Hajmohammad, A. Farrokhian, X. Shen, Slamming impact induced hydrodynamic response in wave-piercing catamaran beam elements with controller, *Ocean Engineering*, Vol. 266, pp. 112908, 2022.

[59] C. Chu, M. Al-Furjan, R. Kolahchi, A. Farrokhian, A nonlinear Chebyshev-based collocation technique to frequency analysis of thermally pre/post-buckled third-order circular sandwich plates, *Communications in Nonlinear Science and Numerical Simulation*, Vol. 118, pp. 107056, 2023.

[60] M. Al-Furjan, Z. Qi, L. Shan, A. Farrokhian, X. Shen, R. Kolahchi, Nano supercapacitors with practical application in aerospace technology: Vibration and wave propagation analysis, *Aerospace Science and Technology*, Vol. 133, pp. 108082, 2023.

[61] P. Wan, M. Al-Furjan, R. Kolahchi, L. Shan, Application of DQHFEM for free and forced vibration, energy absorption, and post-buckling analysis of a hybrid nanocomposite viscoelastic rhombic plate assuming CNTs' waviness and agglomeration, *Mechanical Systems and Signal Processing*, Vol. 189, pp. 110064, 2023.

[62] M. Al-Furjan, S. Fan, L. Shan, A. Farrokhian, X. Shen, R. Kolahchi, Wave propagation analysis of micro air vehicle wings with honeycomb core covered by porous FGM and nanocomposite magnetostrictive layers, *Waves in Random and Complex Media*, pp. 1-30, 2023.

[63] C. Chu, M. Al-Furjan, R. Kolahchi, Energy harvesting and dynamic response of SMA nano conical panels with nanocomposite piezoelectric patch under moving load, *Engineering Structures*, Vol. 292, pp. 116538, 2023.

[64] P. Wan, M. Al-Furjan, R. Kolahchi, Nonlinear flutter response and reliability of supersonic smart hybrid nanocomposite rupture trapezoidal plates subjected to yawed flow using DQHFEM, *Aerospace Science and Technology*, Vol. 145, pp. 108862, 2024.

[65] S. Serdoun, S. Hamza Cherif, Free vibration analysis of composite and sandwich plates by alternative hierarchical finite element method based on Reddy's C1 HSDT, *Journal of Sandwich Structures & Materials*, Vol. 18, No. 4, pp. 501-528, 2016.

[66] J. N. Reddy, 2003, *Mechanics of laminated composite plates and shells: theory and analysis*, CRC press,

[67] S. Ambartsumian, K obshchei teorii anizotropnykh obolochek PMM vol. 22, no. 2, 1958, pp. 226-237, *Journal of Applied Mathematics and Mechanics*, Vol. 22, No. 2, pp. 305-319, 1958.

[68] E. Reissner, On tranverse bending of plates, including the effect of transverse shear deformation, 1974.

[69] R. P. Shimpi, Zeroth-order shear deformation theory for plates, *AIAA journal*, Vol. 37, No. 4, pp. 524-526, 1999.

[70] H. Guenfoud, H. Ziou, M. Himeur, M. Guenfoud, Analyses of a composite functionally graded material beam with a new transverse shear deformation function, *Journal of Applied Engineering Science & Technology*, Vol. 2, No. 2, pp. 105-113, 2016.

[71] A. A. Daikh, A. M. Zenkour, Effect of porosity on the bending analysis of various functionally graded sandwich plates, *Materials Research Express*, Vol. 6, No. 6, pp. 065703, 2019.

[72] R. Kumar, A. Lal, B. Singh, J. Singh, New transverse shear deformation theory for bending analysis of FGM plate under patch load, *Composite Structures*, Vol. 208, pp. 91-100, 2019.

[73] H. Arya, R. Shimpi, N. Naik, A zigzag model for laminated composite beams, *Composite structures*, Vol. 56, No. 1, pp. 21-24, 2002.

[74] A. Zenkour, Analytical solution for bending of cross-ply laminated plates under thermo-mechanical loading, *Composite Structures*, Vol. 65, No. 3-4, pp. 367-379, 2004.

[75] V.-H. Nguyen, T.-K. Nguyen, H.-T. Thai, T. P. Vo, A new inverse trigonometric shear deformation theory for isotropic and functionally graded sandwich plates, *Composites Part B: Engineering*, Vol. 66, pp. 233-246, 2014.

[76] C. H. Thai, S. Kulasegaram, L. V. Tran, H. Nguyen-Xuan, Generalized shear deformation theory for functionally graded isotropic and sandwich plates based on isogeometric approach, *Computers & Structures*, Vol. 141, pp. 94-112, 2014.

[77] C. H. Thai, A. Ferreira, S. P. A. Bordas, T. Rabczuk, H. Nguyen-Xuan, Isogeometric analysis of laminated composite and sandwich plates using a new inverse trigonometric shear deformation theory, *European Journal of Mechanics-A/Solids*, Vol. 43, pp. 89-108, 2014.

[78] S. Suganyadevi, B. Singh, Assessment of composite and sandwich laminates using a new shear deformation theory, *AIAA Journal*, Vol. 54, No. 2, pp. 789-792, 2016.

[79] C. Xiao, G. Zhang, Y. Yu, Y. Mo, R. Mohammadi, Nonlinear vibration analysis of the nanobeams subjected to magneto-electro-thermal loading based on a novel HSDT, *Waves in Random and Complex Media*, pp. 1-20, 2022.

[80] H. Ait Atmane, A. Tounsi, I. Mechab, E. A. Adda Bedia, Free vibration analysis of functionally graded plates resting on Winkler–Pasternak elastic foundations using a new shear deformation theory, *International Journal of Mechanics and Materials in Design*, Vol. 6, pp. 113-121, 2010.

[81] S. Akavci, An efficient shear deformation theory for free vibration of functionally graded thick rectangular plates on elastic foundation, *Composite Structures*, Vol. 108, pp. 667-676, 2014.

[82] M. Karama, K. Afaq, S. Mistou, A new theory for laminated composite plates, *Proceedings of the Institution of Mechanical Engineers, Part L: Journal of Materials: Design and Applications*, Vol. 223, No. 2, pp. 53-62, 2009.

[83] Y. Zhu, P. Shi, Y. Kang, B. Cheng, Isogeometric analysis of functionally graded plates with a logarithmic higher order shear deformation theory, *Thin-Walled Structures*, Vol. 144, pp. 106234, 2019.

[84] F. Pathan, S. Singh, S. Natarajan, G. Watts, An analytical solution for the static bending of smart laminated composite and functionally graded plates with and without porosity, *Archive of Applied Mechanics*, Vol. 92, No. 3, pp. 903-931, 2022.

[85] C. Kumar, R. Kumar, H. K. Sharma, S. Khare, Simulation and Modelling for Bending Analysis of Elastically Supported Laminated Plates Under Concentrated Load: A Meshless Approach, *International Journal of Steel Structures*, Vol. 23, No. 4, pp. 1091-1104, 2023.

[86] M. K. Solanki, R. Kumar, J. Singh, Flexure analysis of laminated plates using multiquadratic RBF based meshfree method, *International Journal of Computational Methods*, Vol. 15, No. 06, pp. 1850049, 2018.

[87] O. Zienkiewicz, J. Zhu, Superconvergence and the superconvergent patch recovery, *Finite elements in analysis and design*, Vol. 19, No. 1-2, pp. 11-23, 1995.

[88] J. E. Akin, 2005, *Finite element analysis with error estimators: An introduction to the FEM and adaptive error analysis for engineering students*, Elsevier,

[89] F. Tornabene, N. Fantuzzi, M. Bacciocchi, J. Reddy, A posteriori stress and strain recovery procedure for the static analysis of laminated shells resting on nonlinear elastic foundation, *Composites Part B: Engineering*, Vol. 126, pp. 162-191, 2017.

[90] L. V. Tran, S.-E. Kim, Static and free vibration analyses of multilayered plates by a higher-order shear and normal deformation theory and isogeometric analysis, *Thin-Walled Structures*, Vol. 130, pp. 622-640, 2018.

[91] J. Reddy, C. Liu, A higher-order shear deformation theory of laminated elastic shells, *International journal of engineering science*, Vol. 23, No. 3, pp. 319-330, 1985.